Shape effects of filaments versus spherical particles in flow and drug delivery

YAN GENG[1†], PAUL DALHAIMER[1†], SHENSHEN CAI[1], RICHARD TSAI[1], MANORAMA TEWARI[1], TAMARA MINKO[2] AND DENNIS E. DISCHER[1*]

[1]NanoBioPolymers and Molecular & Cell Biophysics Lab, University of Pennsylvania, Philadelphia, Pennsylvania 19104, USA
[2]Pharmaceutics, Rutgers University, Piscataway, New Jersey 08854, USA
*e-mail: discher@seas.upenn.edu
†These authors contributed equally to this work.

Published online: 25 March 2007; doi:10.1038/nnano.2007.70

Interaction of spherical particles with cells and within animals has been studied extensively, but the effects of shape have received little attention. Here we use highly stable, polymer micelle assemblies known as filomicelles to compare the transport and trafficking of flexible filaments with spheres of similar chemistry. In rodents, filomicelles persisted in the circulation up to one week after intravenous injection. This is about ten times longer than their spherical counterparts and is more persistent than any known synthetic nanoparticle. Under fluid flow conditions, spheres and short filomicelles are taken up by cells more readily than longer filaments because the latter are extended by the flow. Preliminary results further demonstrate that filomicelles can effectively deliver the anticancer drug paclitaxel and shrink human-derived tumours in mice. Although these findings show that long-circulating vehicles need not be nanospheres, they also lend insight into possible shape effects of natural filamentous viruses.

It is well known that, after intravenous injection, micrometre-sized rigid spheroids are cleared immediately in the first pass through the microvasculature of various bodily organs. Such particles also do not enter most cells. In contrast nanovehicles that are spherically shaped, such as viruses, liposomes or quantum dots, have been widely applied as gene, drug or dye carriers because they tend to circulate *in vivo* for a few hours or perhaps a day (in rodents) and because they can enter cells. Non-spherical nanoparticles have not received significant attention, except perhaps water-soluble carbon nanotubes, which are cleared from the body within hours after intravenous injection[1] and will also enter mammalian cells[2,3]. In nature, a number of viruses that infect animals are likewise filamentous, providing additional motivation for the development and study of soft filamentous vehicles (Fig. 1a; see also Supplementary Information, Fig. S1)[4–6]. Here we examine the distinctive *in vivo* circulation behaviour of such filaments for comparison with spheres of a very similar surface chemistry.

Cylindrically shaped micelles can self-assemble in water from block copolymers that are lipid-like in amphiphilicity[7–9]. However, the copolymers used here are more symmetric than lipids in their hydrophilic/hydrophobic ratio, which leads to the cylindrical shapes. The copolymers are also considerably larger in molecular weight than lipids, which imparts physical stability and aggregate lifetimes of weeks or longer[9]. Our copolymers possess one hydrophilic chain of polyethyleneglycol (PEG), which is widely used to prolong circulation *in vivo*[10–12], and one of two hydrophobic chain chemistries (Table 1): inert polyethylethylene[12] or biodegradable polycaprolactone, which hydrolyses over hours to days in these micelles[13]. The simulation snapshot in Fig. 1a presents a cylinder micelle[14] and two typical configurations of copolymer chains, with hydrophilic blocks in blue and hydrophobic blocks in green. The micellar diameter d_o is controlled primarily by choice of chain molecular weight and varies here from 22 to 60 nm.

Fluorescence labelling and imaging of micelles of several micrometres in length is now straightforward with hydrophobic fluorescent dyes. In addition, controlling the mean length of such soft and fluid assemblies is readily achieved by fragmentation in extrusion through nanoporous filters (Fig. 1a, histogram). By exploiting these methods, we show that PEGylated filomicelles persist in the circulation considerably longer than any known spherical particles. We also show that the filomicelles enter cells under static conditions, but flow opposes entry into cells. All processes prove dependent on the length of filomicelles (requiring stable fluorescence labelling for such assessments) and may lend insight into the possible morphological advantage of natural filoviruses. Additionally, preliminary studies show that filomicelles loaded with the anticancer drug paclitaxel will shrink tumours, with longer cylinders proving more effective at a given dose. The results suggest the promise of filamentous carrier systems, and highlight the effects of shape in biological systems at the nanoscale.

RESULTS AND DISCUSSION

LONG-CIRCULATING FILOMICELLES

Injection of fluorescent filomicelles into the tail veins of rats and mice was followed by fluorescence imaging of blood samples,

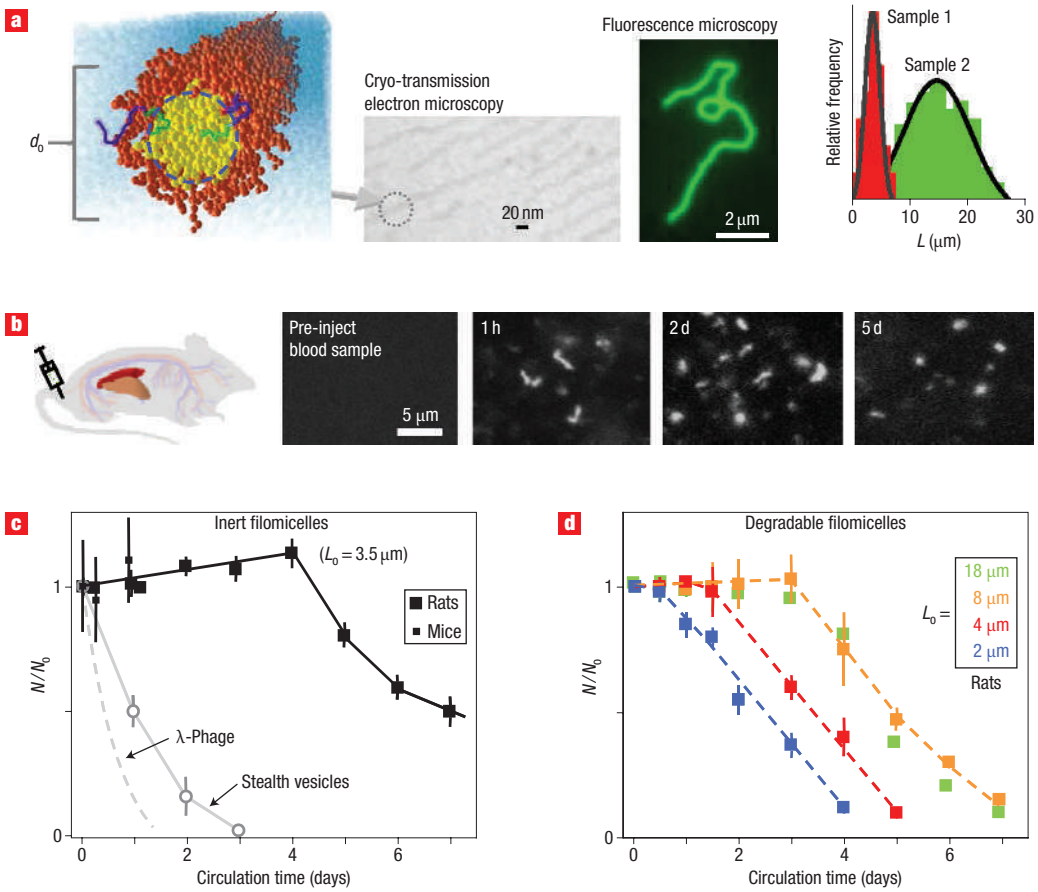

Figure 1 Filomicelles and their persistent circulation. a, Filomicelles are self-assembled from di-block copolymers: yellow/green in cross section indicates hydrophobic polymer, orange/blue is hydrophilic, and aqua is water. Electron microscopy demonstrates the nanometre-scale diameter of the filomicelles[8], and fluorescence microscopy shows a single filomicelle. Distributions of filomicelle length are shown for two samples. **b**, Injection of fluorescent filomicelles into rodents, followed by fluorescent imaging of blood samples showed that filomicelles circulated *in vivo* for up to one week. **c**, Relative numbers of filomicelles in the circulation show that inert filomicelles (of OE7′) persist when compared with stealth polymersomes[12] and λ-phage[16]. **d**, Degradable filomicelles (of OCL3) also persist, and filomicelles with longer initial lengths (L_0) circulate longer up to a limiting length. The error bars in **c**, **d** show the standard deviation for four or more animals.

showing very clearly that a fraction of filomicelles can circulate *in vivo* for up to one week (Fig. 1b–d). The hydrophobic fluorescent dye used in these studies is widely used for long-term cell tracking *in vivo*[15]. We verified with filomicelles in whole blood *in vitro* for one week (at 37 °C) that (1) dye intensity is constant, (2) dye does not transfer to label blood cell membranes, and (3) filomicelles exhibit a constant length distribution. When visualized in blood samples taken from injected mice, filomicelles appear as freely diffusing, distinct and flexible cylinders, and their relative number, N/N_o, in each sample is therefore reliably determined by standard particle-counting image analyses. Persistent circulation is seen for filomicelles that are inert or degradable, and the entire amount injected appears to be dispersed and sustained in the circulation of mice within 1–2 min (see Supplementary Information, Fig. S2). In contrast to the long circulation times of filomicelles, PEGylated 'stealth' vesicles injected at the same dose are cleared within two days (Fig. 1c). Quasi-linear λ-phages with $L \approx 1$ μm are cleared even faster[16]. Circulation of filomicelles also shows a strong dependence on length. Filomicelles of distinct average initial length L_o were made with degradable OCL3 copolymer and injected in multiple animals for parallel studies. For L_o up to ~8 μm, which happens to approximate the diameter of blood cells, longer filomicelles persist longest in the circulation (Fig. 1d).

Filomicelles that exceed an L_o of ~8 μm are shown in the following to undergo rapid fragmentation. Indeed, a weak initial increase in the number of circulating filomicelles followed by the decay in Fig. 1c suggests a general fragmentation process that is eventually dominated by clearance by day 4–5. A mathematical model based on a constant rate of filomicelle scission shows initial increases in N/N_o before removal from the circulation (see Supplementary Information, Fig. S3). Such a mechanism is confirmed by the reduction of filomicelle length as the filaments circulate (Fig. 2a). Fluorescence allows for the measurement of

Table 1 Amphiphilic block copolymers used to make cylindrical filomicelles[15,28].

Copolymer	f_{EO}	Formula	d_o (nm)	l_P (μm)	Degradability
OE7′	0.44	EO_{42}–EE_{35}	25	0.5	Inert
OCL1	0.42	EO_{44}–CL_{24}	22	0.5	Hydrolysable
OCL3	0.43	EO_{110}–CL_{58}	60	5	Hydrolysable

The f_{EO} is the volume fraction of PEG based on NMR, d_o is defined in Fig. 1a as the hydrated diameter, and l_P is the persistence length of the filomicelles, which is longer for stiffer micelles.

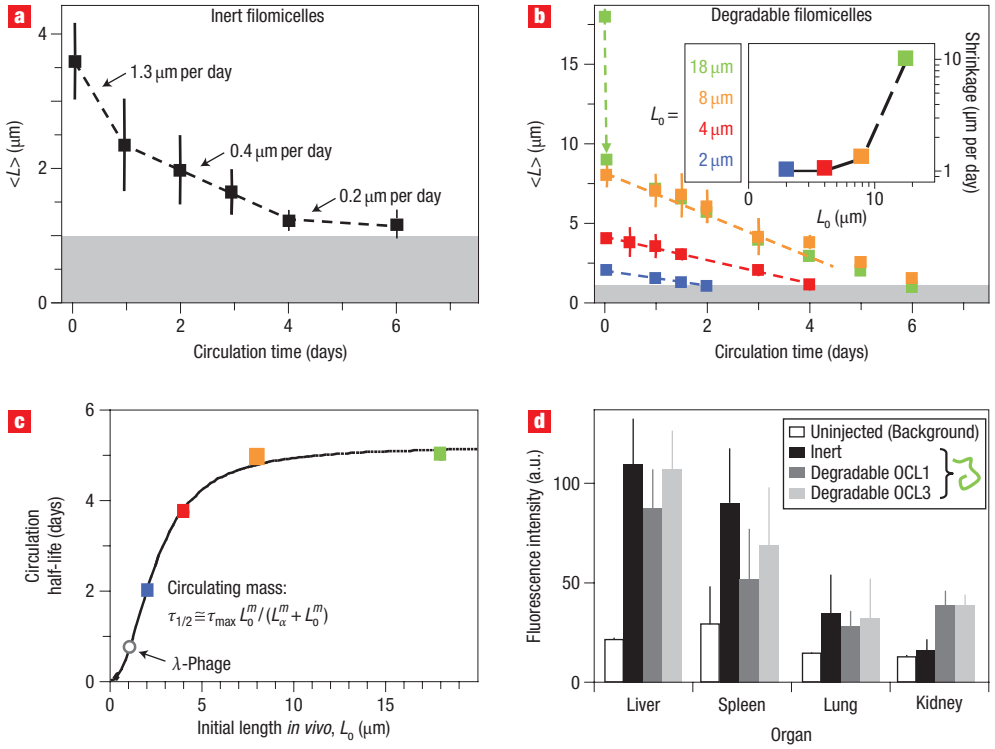

Figure 2 Kinetics of filomicelle length reduction *in vivo*. **a**, Inert filomicelles shorten, with the rate of shortening decreasing as they shorten. The grey region represents the optical limit of *L* measurements. **b**, Degradable filomicelles (OCL3) shorten at a rate that depends on initial length. The inset plots the length-dependent shrinkage rate. **c**, Filomicelles show a saturable increase in half-life of circulating mass, fitting a cooperative clearance model with $\tau_{max} = 5.2$ days, $m = 2.1$ and $L_\alpha = 2.5$ μm. **d**, Distribution of inert and degradable filomicelles in clearance organs for $L_o = 4$ or 8 μm after four days in the circulation of rats. All error bars show the standard deviation for three or more animals.

filomicelle length in each sample (down to an optical resolution of ~0.3 μm) and reveals a progressive decrease in length over one week, even when starting with inert filomicelles of moderate length. The initial shrinkage rate of ~1 μm d^{-1} is due to a combination of cell- and flow-induced fragmentation, and this rate appears to slow with time.

Degradable filomicelles of OCL3 exhibit a similar but more sustained decrease in length (Fig. 2b), which is consistent with progressive shortening by hydrolysis (see Supplementary Information, Fig. S4)[13]. More rapidly degrading OCL1 filomicelles with a diameter similar to that of the inert filomicelles (of the OE7′ copolymer) tend to disappear faster from the circulation (data not shown), which is also consistent with *in situ* hydrolysis. The shortest filomicelles (<4 μm) are seen to shorten somewhat slower than longer filomicelles, and 18-μm (L_o) filomicelles decrease most rapidly, fragmenting to 8 μm after just one hour in circulation. Subsequent circulation proves identical to the 8-μm filomicelles; as noted, this length approximates the diameter of rodent red blood cells, which circulate for many weeks. Because fragmentation does not double the particle numbers (Fig. 1d), the longer segments (of ~10 μm) appear to be cleared from the circulation. Water-soluble nanotubes that are cleared in hours appear to be many micrometres in length (ref. 1), and so the difference here with filomicelles might reflect rigidity more than length. Ebola filoviruses up to 14 μm in length[5] and influenza filaments of at least 20 μm (ref. 17) have been observed.

A simple binding isotherm fit of the circulation results for the filomicelles indicates a maximum half-life of about five days, and implies persistent circulation for soft cylinders with $L_o > 2.5$ μm (Fig. 2c). The mononuclear phagocytic system (MPS) of the liver and the spleen constitutes the usual filtration and clearance pathway for circulating particulates[18,19] and vesicles[12], as well as for the filamentous Ebola and H5N1 viruses[20,21]. Fluorescence imaging of organ slices shows that the liver and spleen also dominate the (slow) clearance of filomicelles (Fig. 2d). The degradable polymer systems (OCL1 and OCL3, Table 1) show somewhat less mass in the spleen and a measurable accumulation in the kidney above tissue autofluorescence levels. The latter appears consistent with hydrolytic degradation leading to molecular-sized products that might permeate the fine mesh of the kidneys. Additionally, moderate accumulation in the lung for all three filomicelle systems might have some relevance to lung infections with both Ebola, which spreads to the lung through the bloodstream[20], and H5N1 influenza, which persists in the lung well after entering the bloodstream[21]. The *in vivo* findings above motivate the *in vitro* studies below of filomicelle interactions with both lung-derived cells and also phagocytic cells that are typical of those found in the liver and spleen.

FILOMICELLES ENTER CELLS BUT EXTEND IN FLUID FLOW

To first address how filomicelles interact with phagocytic cells that are typical of those in the liver or spleen, filomicelles of varying L_o were incubated with activated human-derived macrophages for one day *in vitro*. Previous studies with polymer vesicles prove that such incubation times are adequate for deposition of serum proteins on the PEG brush, thus mediating adhesion of these copolymer systems to phagocytes within seconds of contact[12]. Activated

macrophages incubated with long filomicelles ($\geq 3\,\mu m$) show no fluorescence beyond control macrophages ('no filomicelles' in Fig. 3a). Shorter micelles are, however, taken up by cells, which is evident in an increase in mean cell fluorescence. Plotting the phagocytosis efficiency *versus* micelle length (including results for spherical vesicles) fits a cooperative inhibition model (Fig. 3a, plot), with an effective Hill exponent of $n = 6$ suggesting that multisite attachment occurs between cell and micelle. These results appear qualitatively consistent with the *in vivo* clearance of submicron vesicles and shorter filomicelles, but they do not explain why longer filomicelles ($>2.5\,\mu m$) tend to fragment faster than the shorter micelles.

Because blood in the circulation is in rapid flow and is constantly sheared, vehicles *in vivo* interact with phagocytic cells under fluid dynamic rather than static conditions. Hydrodynamic effects on filomicelles of length $L \gg 1\,\mu m$ are predicted to be strong based on estimates of the dimensionless Weissenberg numbers (Wi) for fluid–polymer interactions near a cell:

$$\mathrm{Wi} = v_{\mathrm{flow}} \tau_{\mathrm{R}} / d_{\mathrm{cell}}$$

where v_{flow} denotes the velocity of blood flow, τ_{R} the relaxation time of a filomicelle and d_{cell} the diameter of a cell. Wi describes the extension of a polymer in flow[22] with two regimes possible: (1) $\mathrm{Wi} > 1$, where the filomicelle cannot relax in the surrounding flow and is stretched out along streamlines, and (2) $\mathrm{Wi} < 1$, where the filomicelle has the shape of a random coil and is able to relax in the flow (that is, rotate and tumble). For the longer filomicelles used here ($L > 1\,\mu m$), τ_{R} has been determined previously to be of order $\sim$1 s (ref. 23). Long filomicelles should be stretched out wherever $v_{\mathrm{flow}} > 5\,\mu m\,s^{-1}$, which includes flow in most blood vessels and also the filtering spleen[24]. This tends to minimize interactions with phagocytes (and surfaces in general). Importantly, because τ_{R} scales with L (ref. 25), shorter cylinders will have lower values for Wi and are expected to interact less with the flow and more with cells, particularly phagocytes.

Flow effects are directly assessed here *in vitro* by steady flow of cylindrical micelles and spherical vesicles past phagocytes. Flow rates similar to those visualized in the spleen[24] are used. When small particles contact the cells, they adhere and appear to be taken up (Fig. 3b, left); however, hydrodynamic shears tend to flow-align the cylindrical filomicelles and pull them off phagocytes as they come into contact (Fig. 3b, right). A nanofragment of a filomicelle might break off and be taken up by the cell, but the strong hydrodynamic force on these long and flexible structures appears to easily overwhelm these cells responsible for filtration and clearance in the body.

Although the filamentous Ebola and Marburg viruses cause haemorrhagic fever and are suspected to interact most strongly with phagocytic cells[5], H5N1 infects the lung[19], which—together with evidence of some lung localization documented in Fig. 2d—motivates a more careful look at interactions with the non-phagocytic cells of the lung. Human lung-derived epithelial cells show an ability to take up fluorescent filomicelles in static culture (Fig. 4a) even though these cells are non-phagocytic, with only a fraction of the uptake efficiency of phagocytes[26]. These lung cells imbibe fluid or pinocytose at least parts of inert filomicelles, which are then trafficked actively to the perinuclear region (see Supplementary Information, Fig. S5), seemingly in a similar way to the trafficking of some microbes by these cells[28]. A time constant of $\tau_{\mathrm{uptake}} \approx 30$ min indicates rapid uptake (Fig. 4b), which saturates before significant deposition of serum protein on the PEG brush is likely to have occurred[12]. Uptake also involves micellar fragmentation, because the filomicelles in the

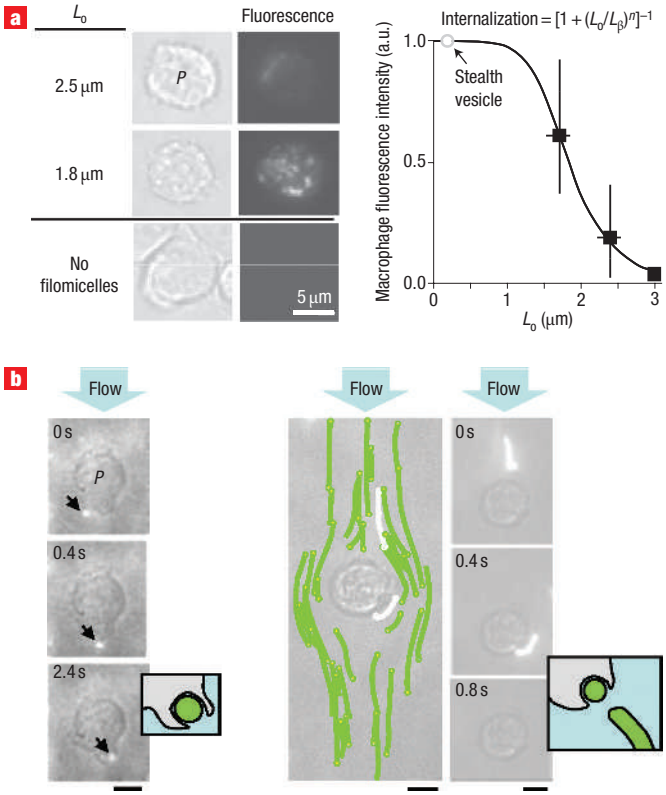

Figure 3 ***In vitro*** **interactions between filomicelles and phagocytes (*P*).** **a**, Fluorescent filomicelles of varying contour length were incubated with activated macrophages for 24 h in static culture. The fluorescence intensity of cells is proportional to the phagocytosis of filomicelles and proves to be a strong function of L_0. The Hill exponent, $n = 6$, suggests strongly cooperative binding along the length of the cylinder to the cell surface. $L_\beta = 1.9\,\mu m$. The error bars in the right-hand plot show the standard deviation. **b**, In a flow chamber with immobilized phagocytes, long filomicelles (right) flow past the cells, and occasionally leave a fragment, but smaller micelles and vesicles are captured (left, arrows point to small micelles and vesicles). Flow velocity is $\sim 25\,\mu m\,s^{-1}$, which is similar to that in the spleen. The scale bars represent 5 μm.

culture supernatant shrink to constant 2.5-μm-long micelles with the same time constant of $\tau_{\mathrm{shrinkage}} \approx 30$ min (Fig. 4c). The calculated shrinkage rate ($\sim 10\,\mu m\,h^{-1}$) suggests that the pinocytosis processes that sever micelles and leave only 2.5-μm-long micelles in the culture supernatant are distinct from phagocytosis processes, where only micelles smaller than 2.5 μm are taken up significantly (Fig. 3a). Based on recent *in vitro* studies of micrometre-sized particles, which show that flattened particles are not readily phagocytosed *en face*[28], it may be that long micelles come into length-wise contact with phagocytes and are similarly perceived. In contrast, internalization by non-phagocytic cells of such length-wise attached micelles seems to recruit motor mechanisms that pinch off smaller endolysosomal vesicles (versus phagosomes), which also fragment the micelles. Regardless of mechanism, the *in vitro* results collectively suggest that multiple processes contribute to shortening of filomicelles, and ultimate clearance *in vivo* is somewhat slower and due primarily to the action of macrophages of the liver and spleen.

In addition to demonstrating strong effects of shape and length on vehicle transport and interactions with cells, we also perturbed the relaxation time τ_{R} (in Wi) by changing the flexibility and

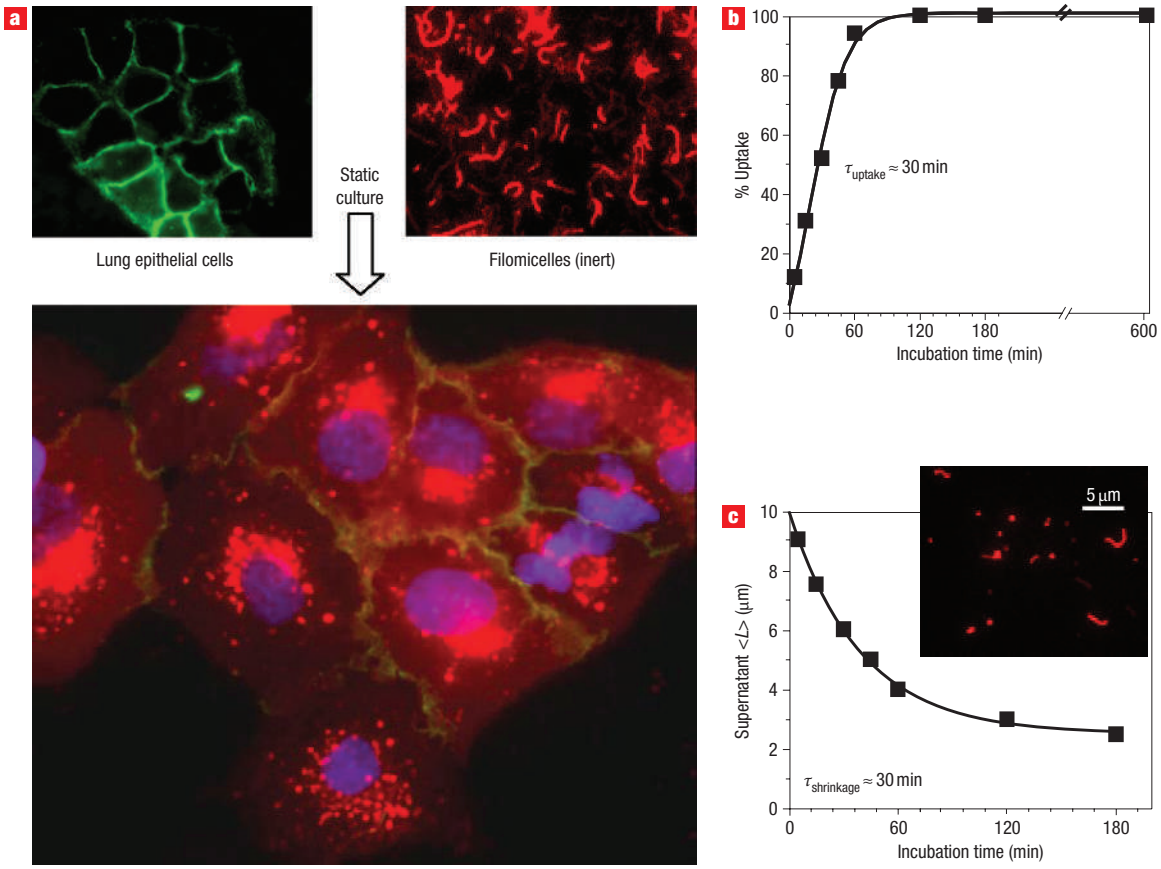

Figure 4 Internalization and fragmentation of filomicelles *in vitro* by human lung-derived epithelial cells. a, Lung cells, prelabelled with a green fluorescent phospholipid probe, were incubated in static cultures with red fluorescent filomicelles. Cell nuclei were later labelled with blue Hoechst dye prior to imaging. **b**, Cellular uptake of filomicelles increases with incubation time, reaching saturation within 1 h. **c**, Remaining filomicelles in the culture supernatant shrink in length on a similar timescale.

fluidity of the filomicelles. Filamentous viruses appear curved or bent and thus suggest the sort of flexibility that has been quantitated as a persistence length l_P with filamentous phages such as M13 ($l_{P,M13} \approx 2\,\mu m$)[29]. Degradable OCL3 micelles are about ten times stiffer ($l_{P,OCL3} \approx 5\,\mu m$)[13] than the inert micelles also studied here, but both circulate for a week or more (Figs 1 and 2) and so flexibility would seem important but weak in its effects. The envelope of filamentous viruses is a flexible fluid lipid bilayer that forms upon budding from cell membranes[30,31], and polymer micelles described here are also fluid along their lengths[23]. To make truly solid cylindrical micelles, crosslinking was introduced into the core of the inert filomicelles (while keeping $l_{P,Xlink}$ low)[23]; on injection, these solid cylinders were found to clear in hours, which is similar to findings for water-soluble, rigid carbon nanotubes of 30–38 nm diameter (ref. 1). Circulation times thus seem set by the ability of a fluid cylinder (micelles and perhaps filoviruses) to relax and/or fragment, either in flow or because of interactions with cells (Figs. 3b and 4).

PACLITAXEL-LOADED FILOMICELLES INDUCE APOPTOSIS AND SHRINK TUMOURS

Persistent circulation has practical applications. Natural viruses are being engineered for their anticancer activity[30,31], as are a broad array of drug-laden, polymer-based spherical micelles[32–34], nanoparticles[35,36], water-soluble nanotubes[1–3] and specialized vesicles[37–41]. Some of the spherical micelles studied recently are even made from an OCL type of copolymer used here in a distinct filamentous shape[34,42]. However, circulation times of all such carriers are generally limited to hours (or up to one day) because of either rapid clearance by the MPS of the liver and spleen or else by excretion. Clinical studies have shown that circulation times of spherical carriers are generally extended threefold in humans over rats[10], so circulation times for filomorphologies could approach one month in humans. As proposed for clinically used drug formulations of PEG-liposomes[11], long-circulating filomicelles would increase the drug exposure to cancer cells and increase the time-integrated dose, commonly referred to in drug delivery as the area under the curve. Additionally, the enhanced permeation and retention effect[33,43] that allows small solutes and micelles to permeate the leaky blood vessels of a rapidly expanding tumour might also allow nanodiameter filomicelles to transport into the tumour stroma. Pioneering developments in phage display have indeed hinted at circulation and permeation of tumours with the filamentous bacteriophage M13 (ref. 44).

To test filomicelles directly as drug-delivery vehicles for cancer therapy, tumour-bearing nude mice[39] were given a single tail-vein injection of either free drug or drug-loaded filomicelle. Saline and empty filomicelles served as control injections. The hydrophobic anticancer drug paclitaxel was injected at the maximum tolerated free drug dose of 1 mg kg^{-1}, or was loaded as recently described[45] at 1 or 8 mg kg^{-1} into the hydrophobic cores of either 1-μm or

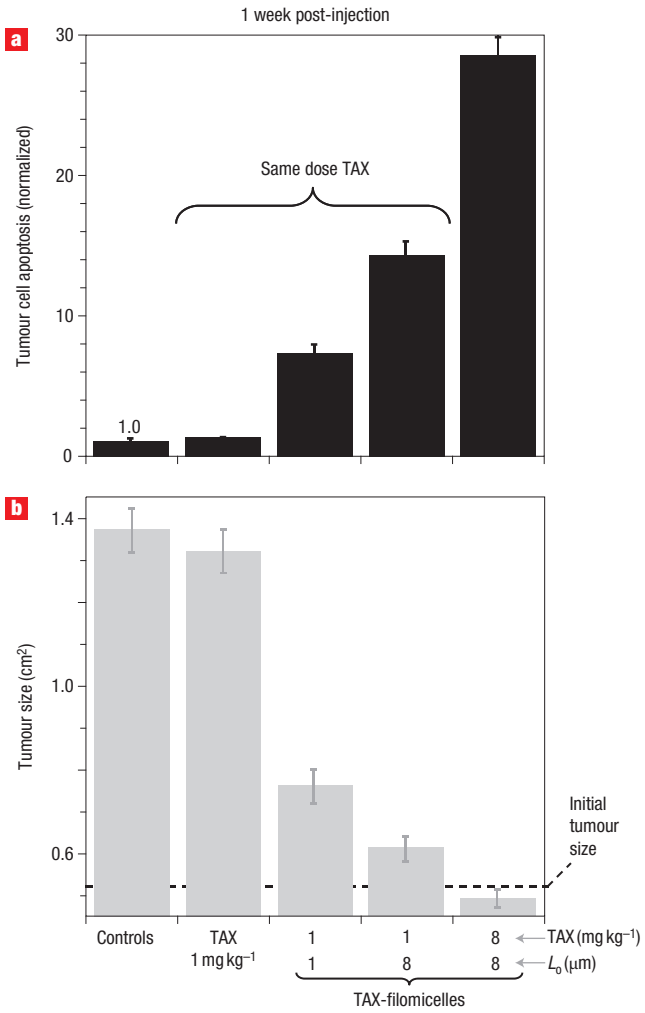

Figure 5 Filomicelles mediate paclitaxel (TAX) delivery to rapidly growing tumour xenografts on nude mice. Tumour-bearing mice were injected with either saline or OCL3 filomicelles as controls, TAX as free drug in ethanol (1 mg kg^{-1} is its maximum tolerated dose), or TAX loaded at two doses into the hydrophobic cores of filomicelles of two lengths. **a**, Apoptosis was measured one week later by quantitative imaging of TUNEL-stained tumour sections and shows little effect of free drug but increasing cell death with increasing L_o and increasing paclitaxel dose. **b**, Tumour size decreases with increasing apoptosis, with tumour shrinkage clear for the longest filomicelles at the highest TAX dose. All data shows the average from four mice. The error bars show the standard deviation.

8-μm filomicelles. Higher doses of drug were not tried, as the intent here was a first comparison of shape and size effects.

Results for filomicelles seven days post-injection demonstrate the clear advantages of the filomicelle as a paclitaxel carrier (Fig. 5). An eightfold increase in filomicelle length for a 1 mg kg^{-1} paclitaxel dosage has about the same relative therapeutic effect as an eightfold increase in the paclitaxel dosage. Both increases lead to a doubling of the apoptosis that is measurable in the tumour, and both increases also lead to a similar relative decrease in tumour size. For comparison, promising phase I clinical trials with paclitaxel-loaded spherical micelles of PEG-(polylactic acid) use approximately an eightfold higher paclitaxel dosage in each of three injections[32]. The present initial tumour studies with filomicelles motivates a deeper understanding of the pharmacokinetics of such soft filamentous vehicles. Our primary goal, however, was to illustrate the strong role of vehicle morphology not only in transport and trafficking, but also perhaps in application.

METHODS

Filomicelles were prepared from hydration of di-block copolymers with no residual co-solvent[13,23]. Block copolymers of PEG-polyethylethylene (EO_m-EE_n, designated OE) or PEG-polycaprolactone (EO_m-CL_n, designated OCL) were synthesized by standard polymerizations[8]; Table 1 provides details of the di-blocks used here. Note that OE7′ is a copolymer related to that used in previous studies of vesicles[12], but the present copolymer has a slightly higher volume fraction of PEG (f_{EO}) that is more consistent with cylinder micelle formation[8] and also with cylinder micelles from the two OCL copolymers with similar f_{EO}. Cryo-transmission electron microscopy allows visualization of the hydrophobic core of the micelles, and the total diameter d_o is estimated to be about twice the core diameter. Filomicelles were visualized by optical microscopy with a hydrophobic membrane marker, PKH26 (Sigma), which partitions into the cores of the filomicelles when added to a hydrated sample[23]. Cell membrane probe, Fluorescein DHPE, nuclei Hoechst stain and Lysotracker Blue were from Molecular Probes.

Fluorescent and bright-field images were recorded using an Olympus IX71 inverted microscope with a CCD camera (Cascade 512, Roper Scientific). Repeated extrusion of filomicelle samples at 100–200 p.s.i. through a 400-nm membrane gently fragments the cylinders, leading under these conditions to a maximum contour length <10 μm, which can be controlled (Fig. 1a, histograms) by the repetitions in extrusion.

For circulation studies, we followed our previous polymer vesicle protocols and assessed performance in two rodent species for comparison with previous studies[12,15,16,18]. Male Sprague–Dawley rats were injected with 0.5 ml of 5 mg ml^{-1} copolymer in phosphate buffered saline; alternatively, equal numbers of male or female C57 mice (with similar results) were injected with 0.1 ml of the same. Orbital bleeds into heparin tubes were taken at various times during the study. The plasma (containing the filomicelles) was separated from the other blood components by centrifugation at 7,000 *g* for 10 min to determine the number, *N*, and contour lengths of the filomicelles in circulation. By comparison to non-centrifuged control samples, this level of centrifugation has no effect on measured length distributions and essentially separates into the supernatant plasma all of the micelles (or vesicles). N_0 is the number of filomicelles from a one-hour bleed for the figures shown. Additional circulation studies in four mice show that (1) filomicelles in blood are statistically the same in number at timepoints of 1–2, 10, 30 and 60 min, and (2) the preinjected concentration is statistically the same as that at 1–2 min when corrected for dilution into the typical blood volume of mice. Organs were retrieved and sectioned (5-μm slices) using a microtome. Each data point in Figs. 1 and 2 represents results from at least 4 rats or mice; organ distribution data in Fig. 3 is from 2–4 rats per condition. In any studies with blood, citrate or EDTA was used as anticoagulant.

In vitro phagocytosis assays were performed on blood-drawn human neutrophils and also a human macrophage cell line, THP1 (ATCC). Filomicelle suspensions of 0.1 mg copolymer (large excess for the number of cells) were incubated with the macrophage cell line for 24 h. *In vitro* assays of internalization of inert filomicelles by human lung-derived cells A549 (ATCC) were performed by incubation of cells prelabelled with fluorescein-phosphatidylethanolamine (FL-DHPE, Molecular Probes) with filomicelles (red dye, PKH26) for preset times. This was followed by removing the supernatant of the remaining filomicelles and washing the cells with PBS three times before imaging. Subsequent fluorescent intensity analysis was used to quantify uptake. Uptake by macrophages depends on activation and is not just a passive adsorption process, as omitting the PMA (phorbol-12-myristate-13-acetate) activation led to cells with control intensities.

Tumour studies were conducted in a similar way to those recently reported[39], with the use here of A549 cells. Briefly, cultured cells were injected subcutaneously onto the backs of nude mice and allowed to grow until they reached a mean size of 0.52 cm^2 ($\pm$0.02 cm^2). Mice were then injected in the tail vein either with saline or filomicelle controls, paclitaxel in ethanol, or the same mass of worm-like filomicelles as above, except that the filomicelles were preloaded with paclitaxel[45]. Each group consisted of four mice. No group of mice showed any significant differences in weight change, and the maximum tolerated dose (MTD) was determined in separate studies to be the dose that causes 10%

weight loss within 24 h (average from three mice). For paclitaxel-loaded filomicelles, the MTD exceeds the 8 mg kg^{-1} used here by more than twofold. For unloaded OCL3 filomicelles (8 μm long), we have injected up to 300 mg kg^{-1} of copolymer without any significant weight loss in mice.

Received 24 October 2006; accepted 2 February 2007; published 25 March 2007.

References

1. Singh, R. *et al.* Tissue biodistribution and blood clearance rates of intravenously administered carbon nanotube radiotracers. *Proc. Natl Acad. Sci. USA* **103,** 3357–3362 (2006).
2. Cai, D. *et al.* Highly efficient molecular delivery into mammalian cells using carbon nanotube spearing. *Nature Methods* **2,** 449–454 (2005).
3. Kam, N. W. S., Dai, H. J. Carbon nanotubes as intracellular protein transporters: Generality and biological functionality. *J. Am. Chem. Soc.* **127,** 6021–6026 (2005).
4. Shortridge, K. F. *et al.* Characterization of avian H5N1 influenza viruses from poultry in Hong Kong. *Virology* **252,** 331–342 (1998).
5. Geisbert, T. W. & Jahrling, P. B. Exotic emerging viral diseases: progress and challenges. *Nature Med.* **10,** S110–S121 (2004).
6. Roberts, P. C., Lamb, R. A., Compans, R. W. The M1 and M2 proteins of influenza A virus are important determinants in filamentous particle formation. *Virology* **240,** 127–137 (1998).
7. Ma, Q., Remsen, E. E., Clark, C. G. Jr., Kowalewski, T., Wooley, K. L. Chemically induced supramolecular reorganization of triblock copolymer assemblies: trapping of intermediate states via a shell-crosslinking methodology. *Proc. Natl Acad. Sci. USA.* **99,** 5058–5063 (2002).
8. Jain, S. & Bates, F. S. On the origins of morphological complexity in block copolymer surfactants. *Science* **300,** 460–464 (2003).
9. Discher, D. E. & Eisenberg, A. Polymer vesicles. *Science* **297,** 967–973 (2002).
10. Gabizon, A., Shmeeda, H. & Barenholz, Y. Pharmacokinetics of pegylated liposomal doxorubicin: review of animal and human studies. *Clin. Pharmacol.* **42,** 419 (2003).
11. Klibanov A. L., Maruyama, K., Torchilin, V. P., & Huang L. Amphipathic polyethyleneglycols effectively prolong the circulation times of liposomes. *FEBS Lett.* **268,** 235–237 (1990).
12. Photos P., Discher, B. M., Bacakova, L., Bates, F. S., Discher, D. E. Polymer vesicles in vivo: correlations with PEG molecular weight. *J. Control Release* **90,** 323–334 (2003).
13. Geng, Y. & Discher, D. E. Hydrolytic shortening of polycaprolactone-*block*-(polyethylene oxide) worm micelles. *J. Am. Chem. Soc.* **127,** 12780–12781 (2005).
14. Srinivas, G., Discher, D. E. & Klein, M. L. Self-assembly and properties of diblock copolymers by coarse-grain molecular dynamics. *Nature Mater.* **3,** 638–644 (2004).
15. Oldenborg, P. A. *et al.* Role of CD47 as a marker of self on red blood cells. *Science* **288,** 2051–2054 (2000).
16. Merril, C. R. *et al.* Long-circulating bacteriophage as antibacterial agents. *Proc. Natl Acad. Sci. USA* **93,** 3188–3192 (1996).
17. Simpson-Holley, M. *et al.* A functional link between the actin cytoskeleton and lipid rafts during budding of filamentous influenza virions. *Virology* **301,** 212–225 (2002).
18. Gref, R. *et al.* Biodegradable long-circulating polymeric nanospheres. *Science* **263,** 1600–1603 (1994).
19. Akerman M. E., Chan, W. C. W., Laakkonen, P., Bhatia, S. N. & Ruoslahti, E. Nanocrystal targeting in vivo. *Proc. Natl Acad. Sci. USA* **99,** 12617–12621 (2002).
20. Baskerville, A., Bowen, E. T., Platt, G. S., McArdell, L. B. & Simpson, D. The pathology of experimental Ebola virus infection in monkeys. *J. Pathol.* **125,** 131–138 (1978).
21. Nishimura, H., Itamura, S., Iwasaki, T., Kurata, T. & Tashiro, M. Characterization of human influenza A (H5N1) virus infection in mice: neuro-, pneumo- and adipotropic infection. *J. Gen. Virol.* **81,** 2503–2510 (2000).
22. Larson, R. G. *The Structure and Rheology of Complex Fluids* (Oxford Univ. Press, New York, 1999).
23. Dalhaimer, P., Bates, F. S. & Discher, D. E. Single molecule visualization of stiffness-tunable, flow conforming worm micelles. *Macromolecules* **36,** 6873–6877 (2003).
24. MacDonald, I. C., Schmidt, E. E. & Groom, A. C. The high splenic hematocrit: a rheological consequence of red cell flow through the reticular meshwork. *Microvasc. Res.* **42,** 60–76 (1991).
25. Doi, M. & Edwards, S. F. *The Theory of Polymer Dynamics* 1st edn (Oxford Univ. Press, Oxford, 1986).
26. Wasylnka, J. A. & Moore, M. M. Uptake of Aspergillus fumigatus Conidia by phagocytic and nonphagocytic cells in vitro: quantitation using strains expressing green fluorescent protein. *Infect. Immunol.* **70,** 3156–3163 (2002).
27. Yavlovich, A., Tarshis, M. & Rottem, S. Internalization and intracellular survival of Mycoplasma pneumoniae by non-phagocytic cells. *FEMS Microbiol. Lett.* **233,** 241–246 (2004).
28. Champion, J. A. & Mitragotri, S. Role of target geometry in phagocytosis. *Proc. Natl Acad. Sci. USA* **103,** 4930–4934 (2006).
29. Song, L., Kim, U. S., Wilcoxon, J. & Schurr, J. M. Dynamic light scattering from weakly bending rods: estimation of the dynamic bending rigidity of the M13 virus. *Biopolymers* **31,** 547–567 (1991).
30. Parato, K. A., Senger, D., Forsyth, P. A. & Bell, J. C. Recent progress in the battle between oncolytic viruses and tumours. *Nature Rev. Cancer* **5,** 965–976 (2005).
31. Mathis, J. M., Stoff-Khalili, M. A. & Curiel, D. T. Oncolytic adenoviruses—selective retargeting to tumor cells. *Oncogene* **24,** 7775–7791 (2005).
32. Kim, T. Y. *et al.* Phase I and pharmacokinetic study of Genexol-PM, a cremophor-free, polymeric micelle-formulated paclitaxel, in patients with advanced malignancies. *Clin. Cancer Res.* **10,** 3708–3716 (2004).
33. Weissig, V., Whiteman, K. R. & Torchilin, V. P. Accumulation of protein-loaded long-circulating micelles and liposomes in subcutaneous Lewis lung carcinoma in mice. *Pharmacol. Res.* **15,** 1552–1556 (1998).
34. Savic, R., Luo, L., Eisenberg, A. & Maysinger, D. Micellar nanocontainers distribute to defined cytoplasmic organelles. *Science* **300,** 615–618 (2003).
35. Hamaguchi, T. *et al.* NK105, a paclitaxel-incorporating micellar nanoparticle formulation, can extend in vivo antitumour activity and reduce the neurotoxicity of paclitaxel. *Br. J. Cancer* **92,** 1240–1246 (2005).
36. Shenoy, D., Little, S., Langer, R. & Amiji, M. Poly(ethylene oxide)-modified poly(beta-amino ester) nanoparticles as a pH-sensitive system for tumor-targeted delivery of hydrophobic drugs: part 2. In vivo distribution and tumor localization studies. *Pharmacol. Res.* **22,** 2107–2114 (2005).
37. Shoji, J., Tanihara, Y., Uchiyama, T. & Kawai, A. Preparation of virosomes coated with the vesicular stomatitis virus glycoprotein as efficient gene transfer vehicles for animal cells. *Microbiol. Immunol.* **48,** 163–174 (2004).
38. Ewert, K., Ahmad, A., Evans, H. M. & Safinya, C. R. Cationic lipid–DNA complexes for non-viral gene therapy: relating supramolecular structures to cellular pathways. *Expert Opin. Biol. Ther.* **5,** 33–53 (2005).
39. Ahmed, F. *et al.* Shrinkage of a rapidly growing tumor by drug-loaded polymersomes: pH-triggered release through copolymer degradation. *Mol. Pharmacol.* **3,** 340–350 (2006).
40. Graff, A., Sauer, M., Van Gelder, P. & Meier, W. Virus-assisted loading of polymer nanocontainer. *Proc. Natl Acad. Sci. USA* **99,** 5064–5068 (2002).
41. Napoli, A., Valentini, M., Tirelli, N., Muller, M. & Hubbell, J. A. Oxidation-responsive polymeric vesicles. *Nature Mater.* **3,** 183–189 (2004).
42. Shuai, X., Ai, H., Nasongkla, N., Kim, S. & Gao, J. Micellar carriers based on block copolymers of poly(epsilon-caprolactone) and poly(ethylene glycol) for doxorubicin delivery. *J. Control Release* **98,** 415–426 (2004).
43. Maeda, H. Enhanced permeability and retention (EPR) effect: basis for drug targeting to tumor. pp. 211–278. In *Biomedical Aspects of Drug Targeting* (eds Muzykantov, V. R. & Torchilin, V. P.) (Kluwer Academic, Boston, 2002).
44. Arap, W., Pasqualini, R. & Ruoslahti, E. Cancer treatment by targeted drug delivery to tumor vasculature in a mouse model. *Science* **279,** 377–380 (1998).
45. Geng, Y. & Discher, D. E. Visualization of degradable worm micelle breakdown in relation to drug release. *Polymer* **47,** 2519–2525 (2006).

Acknowledgements

The authors thank S. Goundla for the simulation snapshot of Fig. 1a, and the Bates Laboratory at the University of Minnesota for OE copolymers. This work was funded by NIH grants (DED), Penn's NSF-MRSEC, NTI, and NSEC (NBIC), and Penn's Institute for Translational Medicine and Therapeutics. Supplementary information accompanies this paper on www.nature.com/naturenanotechnology. Correspondence and requests for material should be addressed to D.E.D.

Author contributions

Y.G. and P.D. contributed equally to this work. Y.G., P.D., T.M. and D.D. conceived and designed the experiments. Y.G., P.D., S.C., R.T., M.T. and T.M. performed the experiments. Y.G., P.D., S.C., R.T., M.T., T.M. and D.D. analysed the data. Y.G., P.D. and D.D. co-wrote the paper.

Competing financial interests

The authors declare that they have no competing financial interests.